

## Paper III



# A Metabolomic Approach to Identify Novel Natural Products from Marine Sponges

*Elisabeth K. Olsen, † Kine L. Söderholm, † Johan Isakson, ‡ Jeanette H. Andersen, § and Espen Hansen\*, §*

†MabCent-SFI, UiT The Arctic University of Norway, N-9037 Tromsø, Norway

‡Department of Chemistry, UiT The Arctic University of Norway, N-9037 Tromsø, Norway

§Marbio, UiT The Arctic University of Norway, N-9037 Tromsø, Norway

\*Authors to whom correspondence should be addressed. Espen Hansen. Tel.: +47 776 49262; Fax: +47-776-46020; e-mail: [espen.hansen@uit.no](mailto:espen.hansen@uit.no)

**Keywords:** Metabolomic, *Geodia barretti*, *Geodia macandrewii*, marine natural products, baretin, N-Acyl-Taurine, Taurine

## Abstract

A metabolomic approach was used to identify known and novel natural products from the marine sponges *Geodia baretii* and *G. macandrewii*. *G. baretii* is known to produce bioactive natural products like baretin, 8,9-dihydrobaretin and bromobenzisoxazolone baretin, while secondary metabolites from *G. macandrewii* are not reported in the literature. Specimens of the two sponges were collected from different sites along the coast of Norway and their extracts were analyzed with UHPLC-HR-MS. Metabolomic analyses revealed that extracts from both species contained baretin and 8,9-dihydrobaretin, and all samples of *G. baretii* contained higher amounts of both compounds compared to *G. macandrewii*. The analysis of the MS data also revealed that samples of *G. macandrewii* contained a compound that was not present in any of the *G. baretii* samples. This was a novel compound identified as an N-Acyl-Taurine and was tested for antioxidant, anticancer and antibacterial properties.

## Introduction

*Geodia barretti* (Bowerbank) is a marine sponge of the class Demospongiae. It is found on continental shelves and slopes of the north Atlantic, and it is common along the coast of Norway at depths between 10 and 500 meters. Specimens of *G. barretti* are irregular in shape, and they can be up to 80 cm in diameter and weigh up to 80 kg<sup>1</sup>. As with many other sponges, the lack of epibionts on the surface of *G. barretti* is striking, and this observation led to the isolation of three structurally related secondary metabolites with anti-fouling properties: baretin, 8,9-dihydrobaretin and bromobenzisoxazolone baretin (Figure 1)<sup>2,3</sup>. As a part of the MabCent screening campaign<sup>4</sup>, extracts of *G. barretti* collected along the coast of Norway were tested in a panel of bioactivity assays, and we found that baretin also had anti-oxidative and anti-inflammatory properties<sup>5</sup>. *G. macandrewii* (Bowerbank) is a related species also commonly found along the coast of Norway. Younger specimen of *G. macandrewii* have spherical bodies which tends to become more irregular when they grow larger than 10 cm in diameter, and they typically reach a size of 35-42 cm (diameter)<sup>1</sup>. There is no records in the literature of bioactive secondary metabolites isolated from *G. macandrewii*.

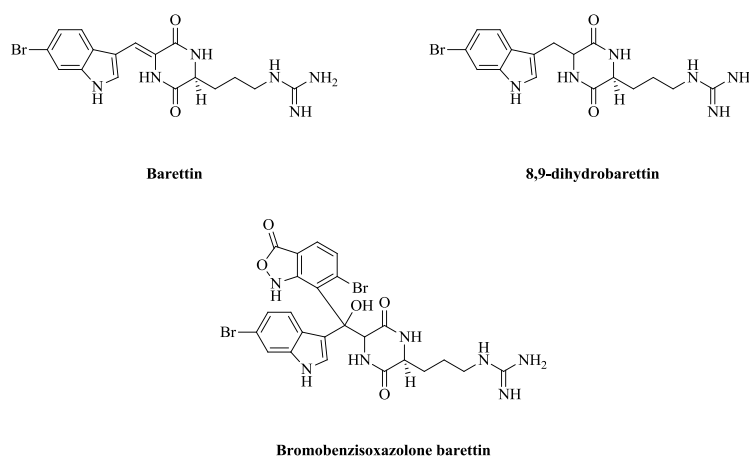


**Figure 1:** Molecular structures of baretin, 8,9-dihydrobaretin and bromobenzisoxazolone.

The MabCent screening campaign has been based on a classic bioassay-guided fractionation approach. Extracts of the marine organisms are prefractionated by HPLC or Flash-chromatography and the fractions are tested for biological activity in a panel of assays. Prefractionation is done to reduce the complexity, e.g. decrease the amount of non-selective compounds and inorganic salts, of crude extracts prior to bioactivity profiling<sup>6</sup>. Any fraction with interesting bioactivity is purified in a series of subsequent fractionation steps, and the bioactivity is traced by screening all fractions in the relevant bioassay<sup>7</sup>. There is a high probability that the isolated compounds have defined bioactivities, but on the other hand it will skew the generated natural products library against the bioactivities selected for the primary screening<sup>8</sup>.

Metabolomics is an alternative approach to detect samples and target compounds for lead identification. This technique can be used to select extracts based on chemical profiling rather than a pre-screened bioactivity. The metabolomics technology is used to identify and quantify molecules in a metabolome, the total of small (< 1500 Da)<sup>9</sup> metabolites or chemicals formed by a cell, tissue, organ or organism, at a specific time and under a specific influence<sup>10-13</sup>. By employing a metabolomics approach an extract can be assessed for chemical novelty or the presence of compounds with specific chemical features<sup>13</sup>. The metabolome can be analyzed using different techniques<sup>10-14</sup>, where mass spectrometry (MS) and nuclear magnetic resonance spectroscopy (NMR) are considered to be the most universal approaches. MS is utilized due to its high sensitivity and that it can detect a wide range of molecular weights, while NMR gives direct structural information about molecular structures<sup>14</sup>.

The current study presents the results from an investigation of two closely related species of sponges, *G. baretii* and *G. macandrewii*, using a metabolomic approach. During a research cruise in 2013, specimens of both species were collected at four different locations along the coast of Norway. By comparing metabolic profiles of the samples we wanted to investigate whether i) both species produced baretin or related compounds, ii) the production of baretin was correlated to sampling location, and iii) *G. macandrewii* produce secondary metabolites not found in *G. baretii*.

## Results and discussion

Sponges were collected on a research cruise at four different locations. Two stations were located in Saltenfjorden in Nordland and two were located in Trondeimsfjorden in Trøndelag. At the stations “Nordland 1” and “Nordland 2” both *G. baretii* and *G. macandrewii* were found, however only *G. baretii* was found at “Trøndelag 1” and “Trøndelag 2”.

The sponges were extracted by a two-step protocol where the samples first were extracted in pure water, and followed by extraction in a mixture of methanol and dichloromethane. This protocol is used by the Developmental Therapeutics Program (DTP) of the National Cancer Institute (Frederick, MD, USA) for the extraction of marine invertebrates<sup>15</sup>. The initial aqueous extraction can be regarded as a purification step as most of the inorganic salts and highly polar compounds such as carbohydrates and amino acids with little interest for drug discovery are efficiently removed from the organic extract. As the overall goal of this study was to identify new potential drug leads the aqueous extracts were not included in the metabolomic analysis.

A combination of ultra-high performance liquid chromatography (UHPLC) and high-resolution mass spectrometry (HR-MS) were used to generate data for the metabolomic analysis. UHPLC-HR-MS is well suited for these kind of analyses as the extracts are complex and contains a wide array of different compounds. The high resolution of the chromatographic separations obtained with this technique makes it possible to separate closely eluting compounds whereas the high resolution of the mass measurements separates compounds with similar masses. To ease the post-acquisition processing of data the analysis was restricted to positive electrospray (ESI+). We are aware of the fact that many acidic and non-polar compounds do not ionize well in ESI+, and that the number of detected compounds could be increased if ESI- was included<sup>16</sup>, although this would have generated a separate data-set. With the parameters applied for collection of markers (i.e. a unique combination of retention time and mass, see experimental section) approximately 500 markers were identified in total.

The metabolic profiles, i.e. the collected markers, for all the samples were compared using a principal components analysis (PCA). The scores plot of the data (Figure 2) revealed that the two *G. macandrewii* samples (M1 and M2) were similar as they grouped closely together, and the same was the case for three of the four samples of *G. baretti* (B1, B2 and B3). The clusters of the two different species were well separated, indicating that there were differences in metabolic profiles. The fourth sample of *G. baretti* (B4) was well separated from the other three samples (B1, B2 and B3), again suggesting that this sample had a unique metabolic profile.

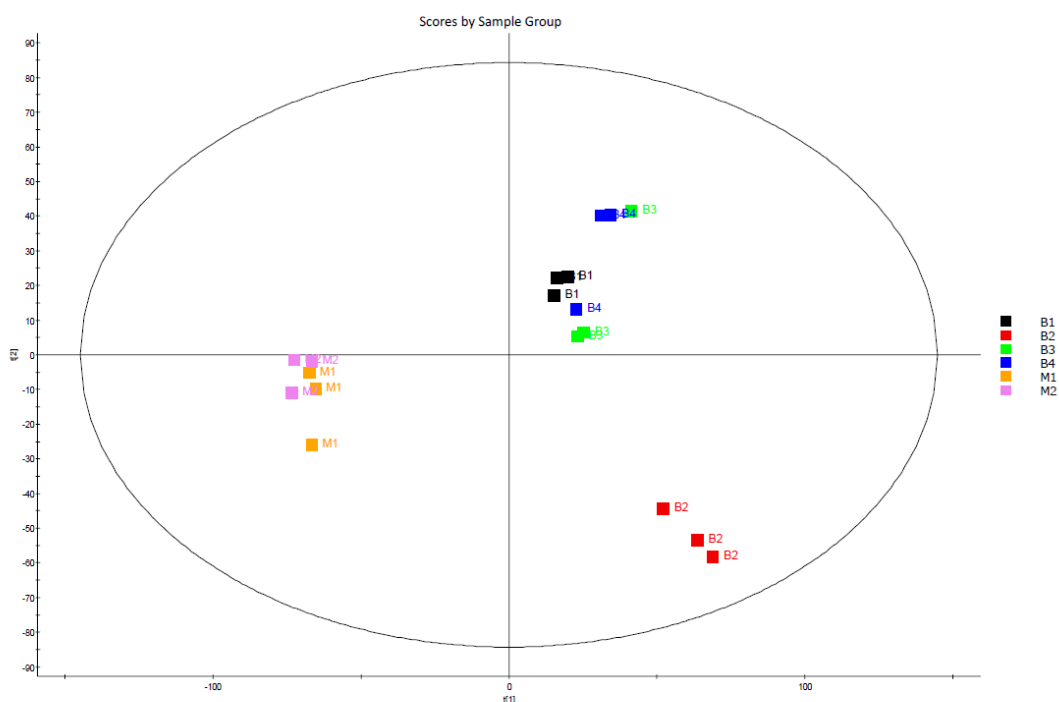


**Figure 2.** A scores plot based on collected markers for two *G. macandrewii* samples (M1 and M2) and four samples of *G. baretti* (B1, B2, B3 and B4).

All samples were found to contain significant amounts of baretin ( $m/z$  419.0829, protonated  $C_{17}H_{20}N_6O_2Br$ ) and 8,9-dihydrobaretin ( $m/z$  421.0988, protonated  $C_{17}H_{22}N_6O_2Br$ ), and the samples of the same species collected at different sites contained similar amounts of both compounds. However, the two samples of *G. macandrewii* contained 80% less baretin and 95 % less 8,9-dihydrobaretin compared to the samples of *G. barretti*. The production of secondary metabolites in sponges are known to vary with both location<sup>17-19</sup> and season<sup>17</sup>. All the samples compared in this metabolomics study were collected at the same cruise and only days apart, thus potential seasonal variations did not affect the data set. Since all samples of *G. barretti* contained more of baretin and 8,9-dihydrobaretin than the *G. macandrewii* samples, the difference in natural products was recognized as species related rather than due to geographical variations. Although our observations indicate that there are no geographical variations between *G. barretti*'s content of the baretins it should be noted that the collection stations of "Nordland" and "Trøndelag" are separated by approx. four degrees of latitude. Hence, sampling of *G. barretti* further distances apart may give different results from those presented here. Baretin has been isolated from *G. barretti* samples collected at different locations along the Swedish<sup>3</sup> and Norwegian coast-line and in the Barents sea<sup>5</sup>, which indicates a wide geographical distribution of this compound.

In order to reveal other differences in the metabolic profiles of the two species, one sample of each species (M1 and B1) were selected and compared in an S-plot. In this plot the x-axis denotes the contribution of a marker to the grouping differences, and the y-axis denotes the confidence of this contribution. Thus the markers in the lower left corner are characteristic for the sample of *G. macandrewii*, whereas the markers in the upper right corner are characteristic for the *G. barretti* sample (Figure 3). The two markers in the upper right corner represent two isomers of baretin ( $m/z$  419 and 421) and the next two represents two isomers of 8,9-dihydrobaretin ( $m/z$  421 and 423). Thus, the main contribution from *G. barretti* to the observed difference in grouping is the higher content of the two related baretin compounds. Even though the data processing is instructed to "deisotope" the data, i.e. to not identify the <sup>13</sup>C-signal from compounds as separate markers, two isotopes of baretin and 8,9-dihydrobaretin are recognized as separate markers because the processing algorithm does not recognize the isotopic pattern of brominated compounds.

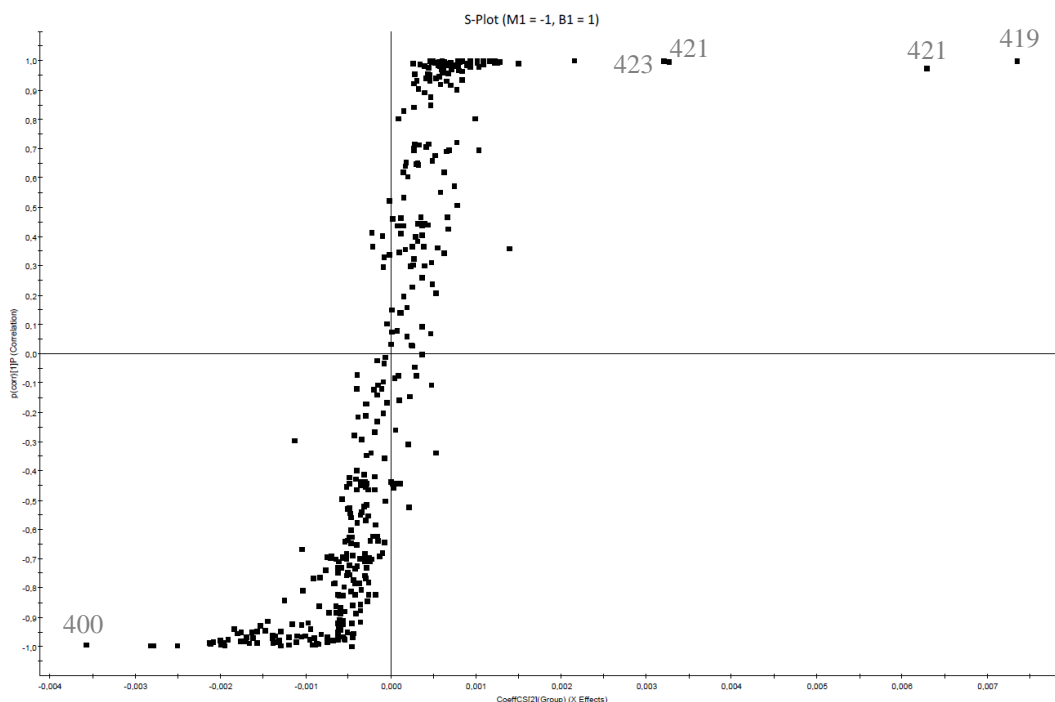


**Figure 3:** An S-plot of one *G. macandrewii* sample (M1) and one *G. baretii* sample (B1). The two isomers of baretin ( $m/z$  419 and 421) and 8,9-dihydrobaretin ( $m/z$  421 and 423) are highlighted. A marker only present in *G. macandrewii*,  $m/z$  400, is also highlighted.

The marker in the lower left corner is the main contribution from *G. macandrewii* to the differences in metabolite profiles. This marker ( $m/z$  400.2473) was not present in any of the *G. baretii* samples although found in equal amounts in both samples of *G. macandrewii*. As no matching compounds was identified in the Dictionary of Marine Natural Products or MarinLit, the compound was isolated and structure elucidated. By using semi-preparative HPLC with mass guided fractionation 0.7 mg of pure compound was isolated from 8.5 g of organic extract.

Compound **1** was isolated as a white amorphous powder. The elemental composition was calculated to be  $C_{21}H_{36}O_4NS$  398.2373 ( $m/z$  398.2373 [M - H]<sup>-</sup>, calculated 398.2371) by using HR-MS in ESI<sup>-</sup>. The <sup>1</sup>H, <sup>13</sup>C NMR and <sup>1</sup>H, <sup>13</sup>C-HSQC spectral data (Figures S3, S4 and S6) indicated the presence of one primary methyl, four vinyl methyls (of which two overlap), six aliphatic methylenes (of which two pairs overlap) and three vinyl methines (all overlap). The spectra also suggested the presence of one carbonyl, one amide and two aliphatic methylenes with moderate downfield shifts ( $\delta_H$  2.51 and 3.31/3.26). The remaining functional groups were attributed to SO<sub>4</sub>H based on the molecular formula, thus implying the presence of a taurine moiety. Three spin systems with a high degree of overlap were observed in the <sup>1</sup>H, <sup>1</sup>H-COSY spectrum (Figure S5), corresponding to CH<sub>3</sub>-CH-CH<sub>2</sub>-CH<sub>2</sub>-CH=, and two -CH<sub>2</sub>-CH<sub>2</sub>-CH= blocks, which implied a repetitive chain. High resolution band selective long range <sup>1</sup>H, <sup>13</sup>C-HMBC correlations (Figure S7-S9) were successfully used to resolve and assign the overlapping carbons to build the chain and attach the vinyl methyl groups. The taurine was then connected to C-2 via the carbonyl ( $\delta_C$  174.77, C-19) based on the following long range couplings: <sup>2</sup>J<sub>C19H20</sub>, <sup>3</sup>J<sub>C19H21</sub>, <sup>2</sup>J<sub>C19H2</sub>, <sup>3</sup>J<sub>C19H1</sub>, <sup>3</sup>J<sub>C19H3</sub>. The geometry of all



the double bonds were all assigned *trans* based on the observed NOESY correlations (Figure S10 and S11): H-7 to H-4/H-9, H-12 to H-9/H-14, H-17 to H-14, and H-18 to H-15. Overlap in both the  $^1\text{H}$  and  $^{13}\text{C}$  dimensions prevented the measurement of the conclusive long range  $^3J_{\text{CH}}$  *trans* couplings individually. Therefore the *trans* assignment could only be confirmed by the absence of any NOESY correlations between the vinyl protons (H-5 and H-10, H-15) and the remaining three vinyl methyls (H-7, H-12 and H-17), which would be observed if the double bonds were *cis*.

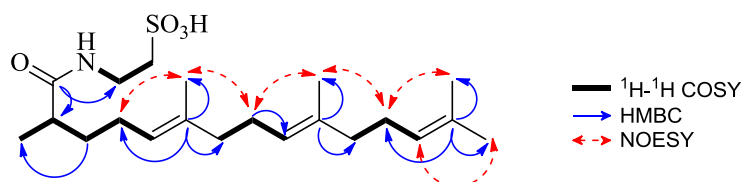


**Figure 4:** Key gHMBC, gCOSY and NOESY correlations of compound 1.

**Table 1:** NMR spectroscopic data<sup>a</sup> (600 MHz,  $\text{dms}\text{-}d_6$ ) for compound 1.

Position	$\delta_{\text{C}}$ , type	$\delta_{\text{H}}$ (J in Hz)	$^1\text{H}$ - $^1\text{H}$ COSY	HMBC
1	17.77, $\text{CH}_3$	0.96 (6.8)	2	
2	39.66, CH	2.13 (7.0)	1, 3	1
3	33.99, $\text{CH}_2$	1.50 (13.2, 6.8) / 1.23	2, 4	1, 4
4	25.34, $\text{CH}_2$	1.86 (8.4, 7.6)	5	5
5	123.92, CH	5.07	4	4, 7
6	134.51, C			4, 7, 8, 9
7	15.73, $\text{CH}_3$	1.53		5, 8
8	39.10, $\text{CH}_2$	1.95-1.90	9	7, 9, 10
9	26.01, $\text{CH}_2$	2.02 (8.0)	8, 10	8, 10
10	123.92, CH	5.07	9	8, 9, 12
11	134.29, C			12, 13, 14
12	17.56, $\text{CH}_3$	1.55		10, 13
13	39.24, $\text{CH}_2$	1.95-1.90	14	12, 14, 15
14	26.19, $\text{CH}_2$	2.02 (8.0)	13, 15	13, 15
15	124.12, CH	5.07	14	13, 14, 17, 18
16	130.61, C			14, 17, 18
17	15.82, $\text{CH}_3$	1.55		18
18	25.50, $\text{CH}_3$	1.63		15, 17
19	174.72, C			1, 2, 3, 20, 21
20		7.65 (5.5)	21	
21	35.41, $\text{CH}_2$	3.32-3.22	20, 22	22
22	50.64, $\text{CH}_2$	2.53 (5.4)	21	21

<sup>a</sup>  $^1\text{H}$ ,  $^{13}\text{C}$ ,  $^1\text{H}$ - $^1\text{H}$  COSY and HMBC spectra are included in the supporting info, Figures S3-S5 and S7.

Compound 1 is a fatty acid amide, composing a fatty acid conjugated to the amino acid taurine, and can be viewed as an N-Acyl-Taurine (NAT)<sup>20</sup>. The fatty acid chain-lengths of NATs vary and they exist as saturated, monounsaturated and polyunsaturated compounds. N-arachidonoyl taurine (C20:4 taurine, N-) and N-oleoyl taurine (C18:1 taurine)<sup>20</sup>, two polyunsaturated NATs first discovered in liver and kidney of fatty acid amide hydrolase (FAAH) knockout mouse<sup>21</sup>, share structural similarities with

compound **1**. Compound **1** differ structurally from both N-arachidonoyl taurine and N-oleoyl taurine in the fatty acid chain length and degree of branching. Whereas N-arachidonoyl taurine and N-oleoyl taurine are non-branched, compound **1** is branched with methyls (Figure 5). The N-arachidonoyl taurine and N-oleoyl taurine are found in mammalian tissue, while there are a few reports of aliphatic NATs having a marine origin. One NAT has been isolated from the sponge *Callyspongia* species<sup>22</sup> and another from the sea urchin *Glyptocidaris crenularis*<sup>23</sup>.

Compound **1**, N-arachidonoyl taurine and N-oleoyl taurine all contain a taurine moiety. Taurine is an amino acid abundant in several different mammalian tissues like brain, retina, spinal cord, leucocytes, heart and muscle cells<sup>24,25</sup>. The physiological functions of taurine are believed to include conjugation of bile acids, maintain osmolality and stabilization membranes<sup>25,26</sup>. Taurine is found to have a cytoprotectant role in the attenuation of apoptosis due to its antioxidant activity<sup>24,27</sup>. The antioxidant activity of taurine has a protective role in the pathology of various diseases like cardiovascular disease<sup>28</sup>, inflammatory diseases<sup>29</sup> and diabetes<sup>24</sup>.

Compound **1** did not exert any antioxidant activity in our cell-based antioxidant assays (CAA and CLPAA), despite the taurine moiety present. The lack of effect may be due to the larger size and/or higher lipophilicity of compound **1** compared to taurine. Other NATs (N-arachidonoyl taurine and N-oleoyl taurine) have previously shown to inhibit proliferation of a prostate and a breast cancer cell line<sup>20</sup>. Bioactivity testing of compound **1** against a melanoma cancer cell line and normal lung fibroblasts showed inhibitory activity in the  $\mu\text{M}$  range. It appears that NATs do not exert a cancer specific inhibitory activity since N-arachidonoyl taurine and N-oleoyl taurine are active against two cancer cell lines, and compound **1** inhibited both melanoma and human lung fibroblasts. Compound **1** did not exert antibacterial activity against either Gram-positive (*S.aureus*, *E.faecalis*, *Streptococcus* gr.B) or Gram-negative (*P.aeruginosa*, *E.coli*) bacteria at 50  $\mu\text{M}$ . Clathrimides A and B, two N-acyl taurine derivatives from the sponge *Clathria compressa* have also previously been shown to be inactive against bacteria<sup>30</sup>.

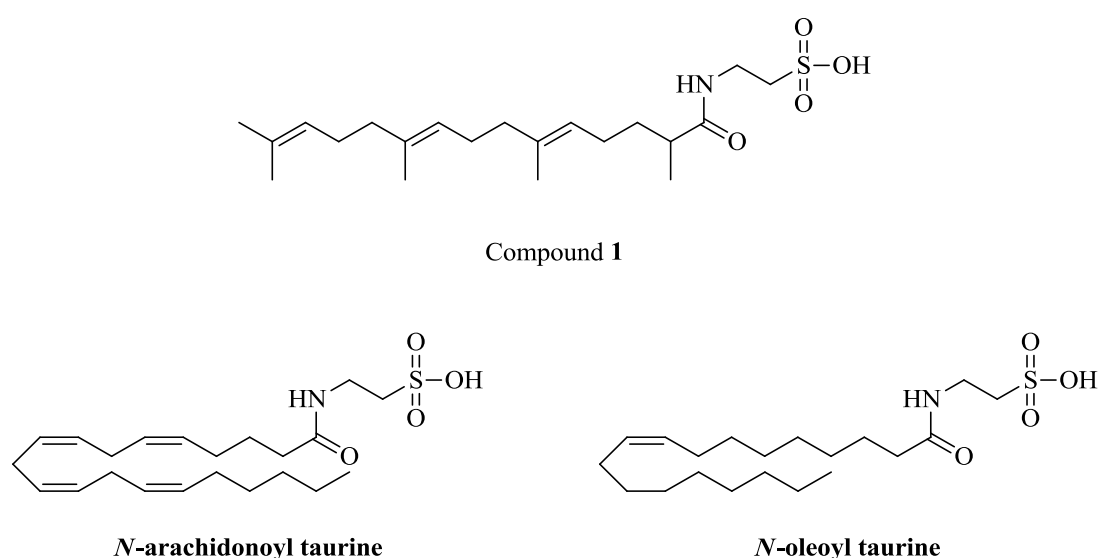


**Figure 5:** Molecular structure of compound **1**. N-arachidonoyl taurine and N-oleoyl taurine are included for structural comparison.

The observed difference between one of the *G. baretii* sample (B2) and the remaining ones (B1, B3 and B4) (Figure 2) in the PCA of the extracts was investigated. The B2 was compared the other three in separate analyses in S-plots of B2 vs. B1, B2 vs. B3 and B2 vs. B4. The marker that contributed most to the observed difference was  $m/z$  524.4306. It was present in all four *G. baretii* samples, although the content was approximately 80% higher in B2. The retention time, accurate mass and elemental composition ( $C_{26}H_{55}NO_7P$   $[M + H]^+$ , calculated 524.3711) correspond to a phosphocholine that we previously have encountered in extracts of several marine sponges. This compound is known to be cytotoxic against human solid tumor cells<sup>31</sup>. As this compound is already well known, it was not pursued for further analysis.

## Conclusion

A novel marine natural product has been isolated and characterized from *G. macandrewii* using a metabolomic approach. This has nicely demonstrated that the bioassay-guided approach to marine natural products drug discovery can be supplemented by other approaches, which rely more on chemometrics and bioinformatics, in order to identify a broad range of compounds. The bioactivities of compounds isolated using the metabolomics might be harder to discover than for those isolated by a bioassay-guided approach. However, metabolomics make valuable additions to natural products screening since libraries of compounds can be established efficiently. Such libraries can be stored and included in new bioassays when available. Both *G. barretti* and *G. macandrewii* contained substantial amounts of baretin and 8,9-dihydrobaretin. Thus enhancing the previous impression that these two compounds are essential, probably as antifouling agents<sup>3</sup>, in sponges.

## Experimental section

**General Experimental Procedures.** Extractions were performed with ultrapure water (Merck Millipore, Darmstadt, Germany), methanol (Chromasolv HPLC grade, Sigma Aldrich, Steinheim, Germany) and dichloromethane (Chromasolv HPLC grade, Sigma Aldrich). UHPLC-HR-MS analyses were done using acetonitrile (Chromasolv LC-MS grade, Sigma Aldrich), ultrapure water and formic acid (LC-MS grade, Sigma Aldrich). Semi-preparative HPLC was done using ultrapure water and acetonitrile (Chromasolv HPLC grade, Sigma Aldrich).

**Collection and extraction of sponges.** Specimens of *Geodia baretii* (Bowerbank, 1858) and *G. macandrewii* (Bowerbank, 1858) were collected by Agassiz trawling at four different locations along the coast of Norway during a sampling cruise with R/V *Helmer Hanssen* in May 2013. The collected specimen were immediately frozen and stored at -22°C until processing in the lab. The frozen sponges were lyophilized, extracted twice in 10x (weight:vol) ultrapure water at 4°C, and centrifuged at 3400 g and 4°C for 30 min. The pellets were subsequently extracted twice in 10x (weight:vol) dichloromethane:methanol (1:1, vol:vol) and vacuum filtrated on Whatman No 1 filters. The pooled organic extracts were reduced to dryness under vacuum in rotary evaporators and stored at -22°C.

**UHPLC-ESI-HR-MS analysis and data processing.** Aliquots of 150 mg of organic extract from each sponge were dissolved in 1.5 mL methanol and centrifuged at 16.000 g for 5 min, and the supernatants were transferred to UHPLC vials. The samples were analyzed by UHPLC-HR-MS on a Waters Acquity UPLC (Milford, MA) coupled to a Waters LCT- Premier time-of-flight MS with electrospray ionization. The sample components were separated on a Waters Acquity ethylene bridged hybrid (BEH) C18 column (2.1 × 150 mm, 1.7 µm) using a gradient of 10-100% acetonitrile in water (both containing 0.1% formic acid) over 10 min and holding for 2 min at 100% acetonitrile with a flow rate of 0.6 mL/min. The column was kept at 40°C, and 1.00 µL of the extracts were injected. The samples were analyzed by positive electrospray ionization, and *m/z* data from 150-1500 were acquired at a scan time of 0.25 sec. Capillary and cone voltages were set at 2.6 kV and 50 V, respectively, while source and desolvation temperatures were set to 120°C and 350°C, respectively. Nitrogen was used as desolvation gas at 500 L/min. The MS was tuned to a resolution of 10,000 (FWHM), and leucine-enkephaline was infused through the reference probe for internal calibration during data acquisition.

**Post-acquisition data processing.** The HR-MS data were analyzed using MassLynx 4.1 and the MarkerLynx application manager (Waters). Markers between 150 and 1500 Da were collected with an intensity threshold of 500 counts and retention time and mass windows of 0.2 min and 0.1 Da, respectively. The noise level was set to 10.00 and the raw data were deisotoped. Statistical analysis of the data was done using EZinfo 2.0 (Umetrics, Umeå, Sweden).

**Isolation of compound 1.** The compound was isolated using a Waters auto purification system consisting of a 2767 sample manager, 600E pump, 2996 photodiode array detector and 3100 mass detector. 4 g of the organic extract were dissolved in 200 ml hexane, and extracted twice with 90% aqueous acetonitrile. The acetonitrile phases

were combined, reduced to dryness under vacuum in a rotary evaporator, dissolved in 90% methanol, and 500  $\mu$ L aliquots were injected onto a Waters Atlantis Prep C18 column (10  $\times$  250 mm, 10  $\mu$ M). Acetonitrile and 10 mM ammonium formate (pH 8) were used as mobile phases at a low rate of 6 ml/min. Compound **1** was isolated using a gradient of 45-55 % acetonitrile over 10 minutes with  $m/z$  400.2 as fraction collection trigger (positive electrospray).

**NMR.** All NMR spectra were acquired on a Varian inova spectrometer operating at 599.924 MHz for  $^1\text{H}$  and 150.867 MHz for  $^{13}\text{C}$ , equipped with a cryogenically enhanced inverse triple resonance HCN probe. Experiments were typically acquired with presaturation on the water resonance, gradient selection and adiabatic/BIP versions where applicable. Experiment list: 1D  $^1\text{H}$ , 1D  $^{13}\text{C}$ , DQFCOSY, NOESY (300 ms, ZQ filtered), ROESY (200 ms, adiabatic), HSQC (146 and 125 Hz, BIP, SE), HMBC (8 Hz, BIP), band selective HMBC (8 Hz, 10-50 and 120-140 ppm). Spectra were calibrated on the residual solvent peak of dms- $d_6$  ( $\delta_{\text{H}}=2.50$  ppm,  $\delta_{\text{C}}=49.52$  ppm). Data was processed, and multiplets and chemical shifts were simulated in Mnova v9.0.1-13254.

**Structure elucidation of compound 1.** White amorphous powder;  $^1\text{H}$  NMR (600 MHz, dms- $d_6$ )  $\delta_{\text{H}}$  7.65 (1H, t,  $J = 5.5$  Hz, H-20), 5.07 (3H, o, H-5, H-10, H-15), 3.28 (1H, m, H-21), 2.51 (2H, o, H-22), 2.13 (1H, h,  $J = 6.7$  Hz, H-2), 2.06-1.99 (4H, o, H-9, H-14), 1.95 – 1.90 (4H, m, H-8, H-13), 1.86 (2H, dd,  $J = 8.0, 7.5$  Hz, H-4), 1.63 (3H, s, H-18), 1.55 (6H, o, H-12, H-17), 1.53 (3H, s, H-7), 1.49 (1H, m, H-3'), 1.23 (1H, o, H-3''), 0.96 (3H, d,  $J = 6.8$  Hz, H-1);  $^{13}\text{C}$  NMR (151 MHz, dms- $d_6$ )  $\delta_{\text{C}}$  174.77 (C-19), 134.52 (C-6), 134.30 (C-11), 130.63 (C-16), 124.12 (C-15), 123.92 (C-5), 50.65 (C-22), 39.61 (C-2), 39.19 (C-13), 39.16 (C-8), 35.43 (C-21), 34.00 (C-3), 26.19 (C-14), 26.04 (C-9), 25.52 (C-18), 25.36 (C-4), 17.77 (C-1), 17.58 (C-12), 15.84 (C-17), 15.74 (C-7); HRESIMS  $m/z$  398.2373 [ $\text{M}]^-$  (calcd for  $\text{C}_{21}\text{H}_{36}\text{NO}_4\text{S}^-$ , 398.2371).

**Bioactivity testing.** A stock solution of **1** in DMSO (20 mg/mL) was prepared for compound **1**.

*Cell viability.* A working solution of **1** was prepared by diluting the stock solution in RPMI-1640 (FG1385, Biochrom) added gentamycin (10  $\mu\text{g/mL}$ , A2712, Biochrom). Cells added RPMI with gentamycin was used as a negative control while cells treated with Triton<sup>®</sup> X-100 (T8787, sigma aldrich) was used as a positive control. A2058 (human, melanoma; ATCC, CRL-11147<sup>TM</sup>) was cultivated in D- MEM (32430-027, Gibco) with fetal bovine serum (10%, S0115, Biochrom) and MRC-5 (human fetal lung; ATCC, CCL-171<sup>TM</sup>) was cultivated in MEM-Earle's medium (F0325, Biochrom) supplemented with fetal bovine serum (10%), stable L-glutamine (2 mM, K0302, Biochrom) non-essential amino acids (1%, K0293, Biochrom), sodium pyruvate (1 %, L0473, Biochrom) and  $\text{NaHCO}_3$  (2%, L1713. Biochrom). Cells were seeded in a 96-well microtiter plate (Nunc 167008) in RPMI-1640 with 10% FBS, at a concentration of approximately 2000 cells/well for A2058 cells/well and 4000 cells/well for MRC-5. The plate was incubated for 24 hours before the medium was removed and replaced with RPMI-1640 added FBS (10%) and gentamycin (10  $\mu\text{g/mL}$ ), and **1** added in triplicates. After 72 h incubation CellTiter 96<sup>®</sup> AQueous One Solution Reagent (Promega, Madison, WI, USA) was added and the plate incubated for one hour before absorbance at 485 nm was read. All incubations were done at 37  $^\circ\text{C}$  in a humidified atmosphere of 5%  $\text{CO}_2$ . The total reaction volume was 100  $\mu\text{L}$ .

*Inhibition of bacterial growth.* A working solution of **1** was prepared by diluting the stock solution in milliQ H<sub>2</sub>O. The antibacterial activity was tested on 5 different strains; *E.faecalis* (ATCC 29212), *E.coli* (ATCC 25922), *P.aeruginosa* (ATCC 27853), *S.aureus* (ATCC 25923) and *Streptococcus* B (ATCC 12386). Growth medium with sterile milliQ H<sub>2</sub>O was used as a negative control while sterile milliQ H<sub>2</sub>O and bacteria suspension was used as a positive control. Bacteria were transferred from a blood plate to growth medium (MH-bullion (VL787693 717, Merck) for *E.coli*, *P.aeruginosa* and *S.aureus* and BHI-bullion (CM1135, OXOID) for *E.faecalis* and *Streptococcus* gr. B) and incubated at 37°C overnight. The following day a part of the bacteria suspension was transferred to fresh medium and cultivated in a shaker incubator at 37°C for 1,5 h (*E.coli*, *E.faecalis* and *Streptococcus* gr. B) or 2,5 h (*S.aureus* and *P.aeruginosa*). The bacteria suspension was then diluted 1:100 in medium and added all wells in a 96-well microtiter plate (Nunc 167008), followed by **1** in duplicates. The plates were incubated at 37°C overnight before growth was controlled visually and photometrical at 600 nm. The total reaction volume was 100 µL.

*Antioxidant activity.* A working solution of **1** was prepared by diluting the stock solution in milliQ H<sub>2</sub>O. The antioxidant activity of **1** was explored using two cellular assays: the Cellular Antioxidant Activity (CAA) and Cellular Lipid Peroxidation Antioxidant Activity (CLPAA) assays. The assays were performed as previously reported by our research group<sup>32</sup>.

#### ASSOCIATED CONTENT

**Supporting Information.** HR-MS data, 1D and 2D NMR compound **1**.

#### AUTHOR INFORMATION

##### **Corresponding Author**

\*Espen Hansen Tel: +47 77649262. Fax: +47-776-46020; e-mail: [espen.hansen@uit.no](mailto:espen.hansen@uit.no)

##### **Author Contributions**

The manuscript was written through contributions of all authors. All authors have given approval to the final version of the manuscript.

#### ACKNOWLEDGMENT

The authors would like to thank Marbank for providing the *G. barretti* and *G. macandrewii* samples. This work was supported by MabCent-SFI, centre for research based innovation the University of Tromsø, supported by the Research Council of Norway (Grant no 174885/130).

## REFERENCES

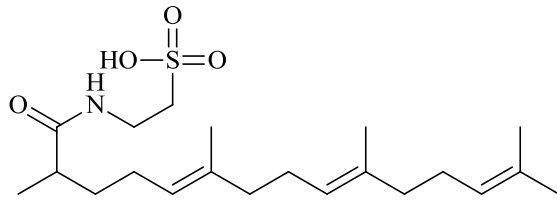
- (1) Cardenas, P.; Rapp, H. T.; Klitgaard, A. B.; Best, M.; Thollesson, M.; Tendal, O. S. *Zool J Linn Soc* **2013**, *169*, 251.
- (2) Hedner, E.; Sjogren, M.; Hodzic, S.; Andersson, R.; Goransson, U.; Jonsson, P. R.; Bohlin, L. *J Nat Prod* **2008**, *71*, 330.
- (3) Sjogren, M.; Goransson, U.; Johnson, A. L.; Dahlstrom, M.; Andersson, R.; Bergman, J.; Jonsson, P. R.; Bohlin, L. *J Nat Prod* **2004**, *67*, 368.
- (4) Svenson, J. *Phytochem Rev* **2013**, *12*, 567.
- (5) Lind, K. F.; Hansen, E.; Osterud, B.; Eilertsen, K. E.; Bayer, A.; Engqvist, M.; Leszczak, K.; Jorgensen, T. O.; Andersen, J. H. *Mar. Drugs* **2013**, *11*, 2655.
- (6) Camp, D.; Davis, R. A.; Campitelli, M.; Ebdon, J.; Quinn, R. J. *J Nat Prod* **2012**, *75*, 72.
- (7) Weller, M. G. *Sensors* **2012**, *12*, 9181.
- (8) Rollinger, J. M.; Langer, T.; Stuppner, H. *Curr Med Chem* **2006**, *13*, 1491.
- (9) Di Lena, M.; Travaglio, E.; Altomare, D. F. *Colorectal Dis* **2014**, *16*, 235.
- (10) Ulrich-Merzenich, G.; Zeitler, H.; Jobst, D.; Panek, D.; Vetter, H.; Wagner, H. *Phytomedicine* **2007**, *14*, 70.
- (11) Colquhoun, I. J. *J Pestic Sci* **2007**, *32*, 200.
- (12) Verpoorte, R.; Choi, Y. H.; Kim, H. K. *Phytochem. Rev.* **2007**, *6*, 3.
- (13) Yuliana, N. D.; Khatib, A.; Choi, Y. H.; Verpoorte, R. *Phytother Res* **2011**, *25*, 157.
- (14) Verpoorte, R.; Choi, Y. H.; Mustafa, N. R.; Kim, H. K. *Phytochem. Rev.* **2008**, *7*, 525.
- (15) McCloud, T. G. *Molecules* **2010**, *15*, 4526.
- (16) Nordstrom, A.; Want, E.; Northen, T.; Lehtio, J.; Siuzdak, G. *Anal Chem* **2008**, *80*, 421.
- (17) Abdo, D. A.; Motti, C. A.; Battershill, C. N.; Harvey, E. S. *J Chem Ecol* **2007**, *33*, 1635.
- (18) Noyer, C.; Thomas, O. P.; Becerro, M. A. *PLoS ONE* **2011**, *6*, e20844.
- (19) Sacristan-Soriano, O.; Banaigs, B.; Becerro, M. A. *Mar. Drugs* **2011**, *9*, 2499.
- (20) Chatzakos, V.; Slätis, K.; Djureinovic, T.; Helleday, T.; Hunt, M. *Lipids* **2012**, *47*, 355.
- (21) Saghatelian, A.; McKinney, M. K.; Bandell, M.; Patapoutian, A.; Cravatt, B. F. *Biochemistry* **2006**, *45*, 9007.
- (22) Huang, R.; Chen, Y.; Zhou, X.; Yang, X.; Liu, Y. *Chem Nat Compd* **2015**, *51*, 540.
- (23) Zhou, X.; Xu, T.; Wen, K.; Yang, X.-W.; Xu, S.-H.; Liu, Y. *Biosci, Biotechn, and Biochem* **2010**, *74*, 1089.
- (24) Ripps, H.; Shen, W. *Molecular Vision* **2012**, *18*, 2673.
- (25) Timbrell, J. A.; Seabra, V.; Waterfield, C. J. *Gen Pharmacol- vasc s* **1995**, *26*, 453.
- (26) Hansen, S. H. *Diabetes Metab Res Rev* **2001**, *17*, 330.
- (27) Jong, C.; Azuma, J.; Schaffer, S. *Amino Acids* **2012**, *42*, 2223.
- (28) Chen, G.; Nan, C.; Tian, J.; Jean-Charles, P.; Li, Y.; Weissbach, H.; Huang, X. P. *J Cell Biochem* **2012**, *113*, 3559.

- (29) Marcinkiewicz, J.; Kontny, E. *Amino Acids* **2014**, *46*, 7.
- (30) Gupta, P.; Sharma, U.; Schulz, T. C.; McLean, A. B.; Robins, A. J.; West, L. M. *J Nat Prod* **2012**, *75*, 1223.
- (31) Alam, N.; Bae, B. H.; Hong, J.; Lee, C. O.; Shin, B. A.; Im, K. S.; Jung, J. H. *J Nat Prod* **2001**, *64*, 533.
- (32) Olsen, E.; Hansen, E.; Isaksson, J.; Andersen, J. *Mar. Drugs* **2013**, *11*, 2769.



## Table of content graphic

©Bjørn Gulliksen.



**Supporting Information, Paper III**

# A Metabolomic Approach to Identify Novel Natural Products from Marine Sponges

*Elisabeth K. Olsen, † Kine L. Söderholm, † Johan Isakson, ‡ Jeanette H. Andersen, § and Espen Hansen\*, §*

†MabCent-SFI, UiT The Arctic University of Norway, N-9037 Tromsø, Norway

‡Department of Chemistry, UiT The Arctic University of Norway, N-9037 Tromsø, Norway

§Marbio, UiT The Arctic University of Norway, N-9037 Tromsø, Norway

## Contents

**Figure S1.** High-resolution MS spectrum of **1**

**Figure S2.** A correlation plot of compound **1** between neural network based predicted chemical shifts and experimental chemical shifts for  $^{13}\text{C}$ .

**Figure S3.**  $^1\text{H}$ -NMR spectrum of **1** in  $\text{dms}\text{-}d_6$ .

**Figure S4.**  $^{13}\text{C}$ -NMR spectrum of **4** in  $\text{dms}\text{-}d_6$ .

**Figure S5.**  $^1\text{H}$ ,  $^1\text{H}$ -COSY (gcosy) spectrum of compound **1** in  $\text{dms}\text{-}d_6$ .

**Figure S6.** HSQC (gc2hsqcse) spectrum of compound **1** in  $\text{dms}\text{-}d_6$ .

**Figure S7.** HMBC (gc2hmhc) of compound **1** in  $\text{dms}\text{-}d_6$ .

**Figure S8.** High resolution band selective gradient HMBC (bsghmhc) (10-50 ppm) of compound **1** in  $\text{dms}\text{-}d_6$ .

**Figure S9.** High resolution band selective gradient HMBC (bsghmhc) (120-140 ppm) of compound **1** in  $\text{dms}\text{-}d_6$ .

**Figure S10.** 300 ms NOSEY spectrum of compound **1** in  $\text{dms}\text{-}d_6$ .

**Figure S11.** 300 ms NOSEY spectrum of compound **1** in  $\text{dms}\text{-}d_6$  (0.5-2 ppm)

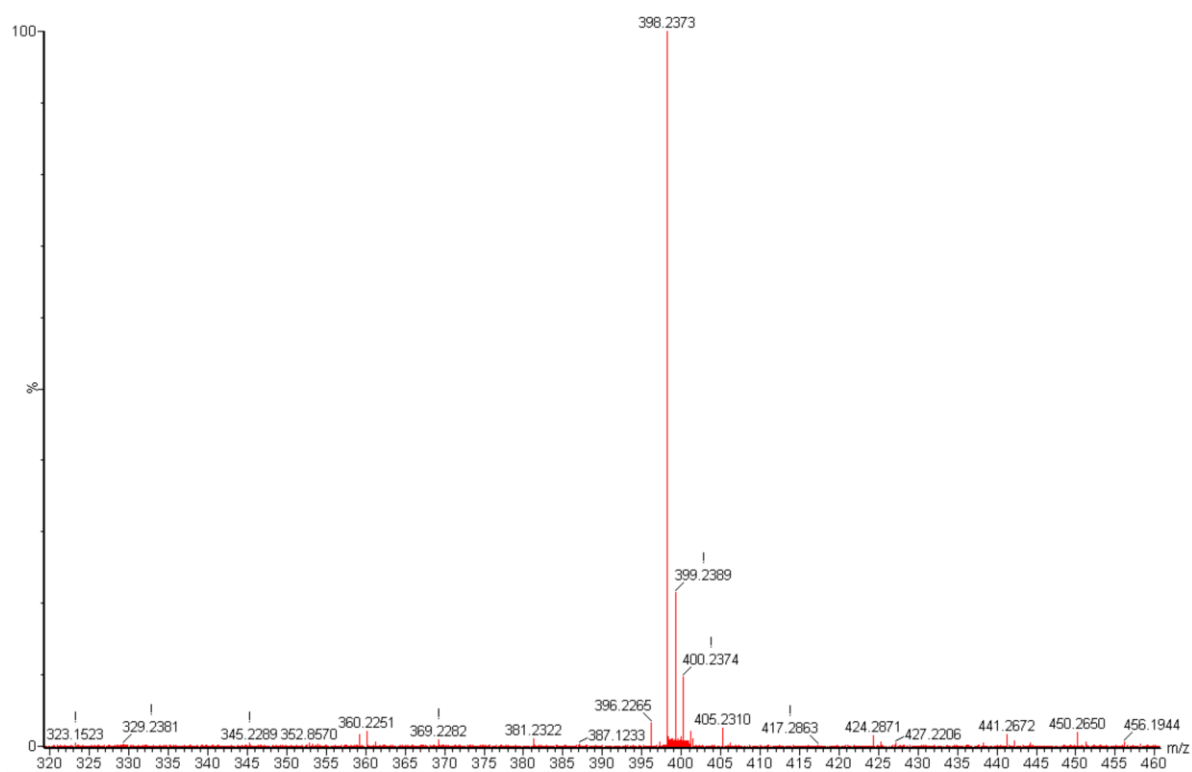


**Figure S1.** High-resolution MS spectrum of **1**

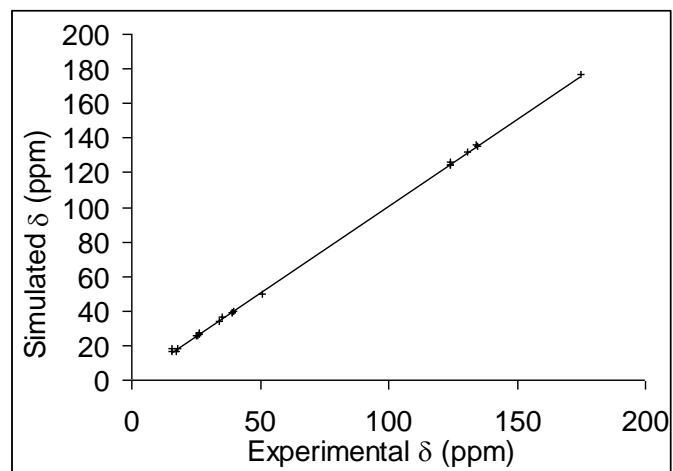


**Figure S2.** A correlation plot between neural network based predicted chemical shifts and experimental chemical shifts for  $^{13}\text{C}$ , mean error: 0.81 ppm,  $r^2=0.9998$ .

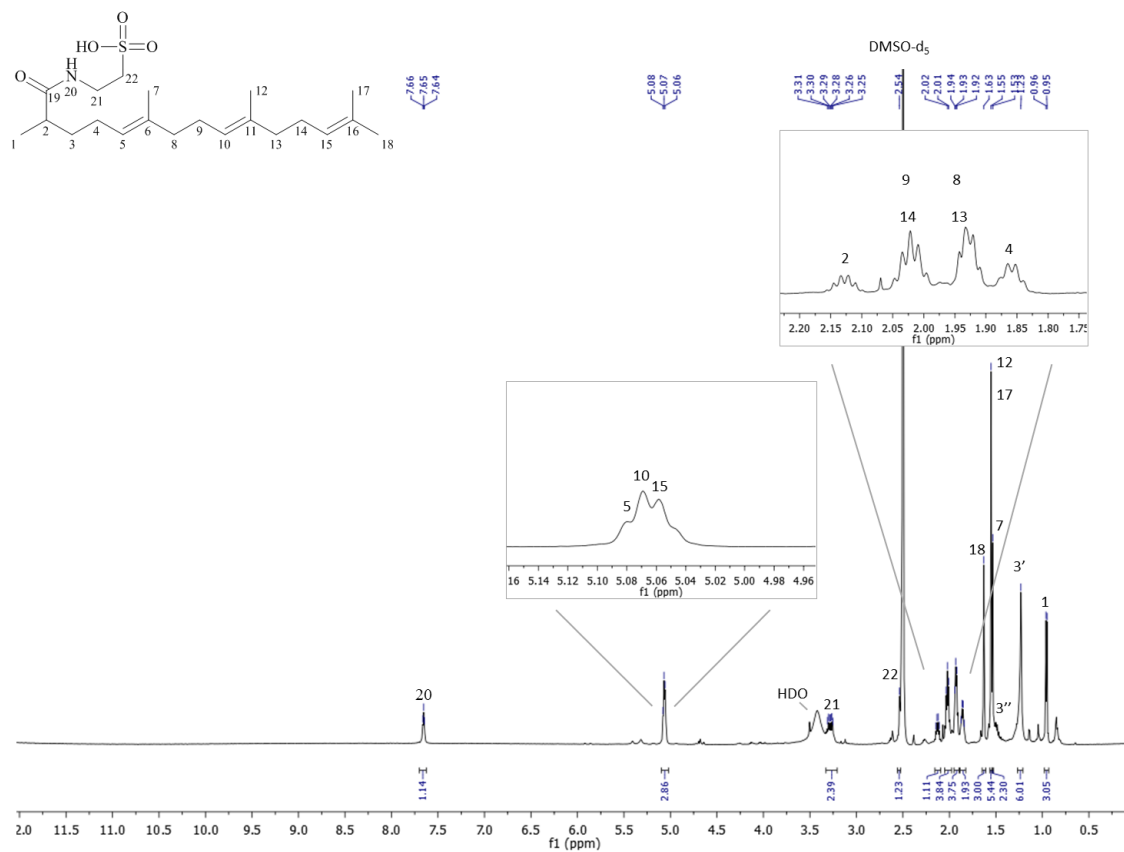


**Figure S3.**  $^1\text{H-NMR}$  spectrum (Presat) of compound **1** in  $\text{dmsO-}d_6$ , with presaturation on the water signal.

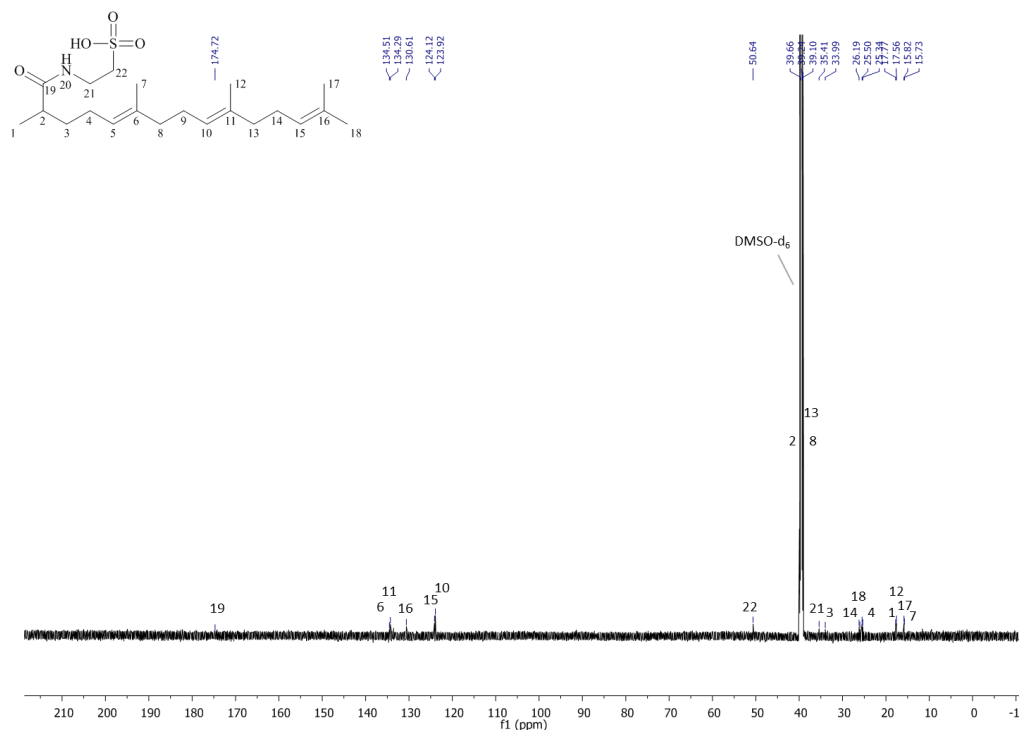


**Figure S4.** <sup>13</sup>C-NMR spectrum of compound 1 in dmsO-d<sub>6</sub>.

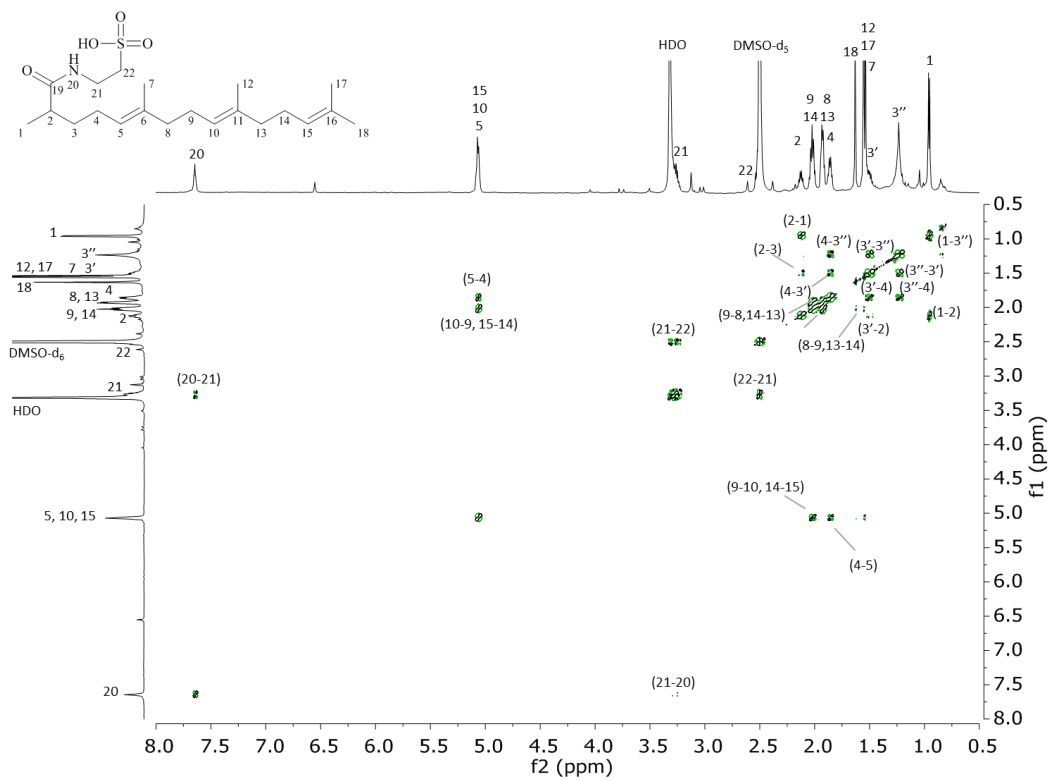


**Figure S5.**  $^1\text{H}$ ,  $^1\text{H}$ -COSY (gcosy) spectrum of compound **1** in  $\text{dms0-d}_6$ .



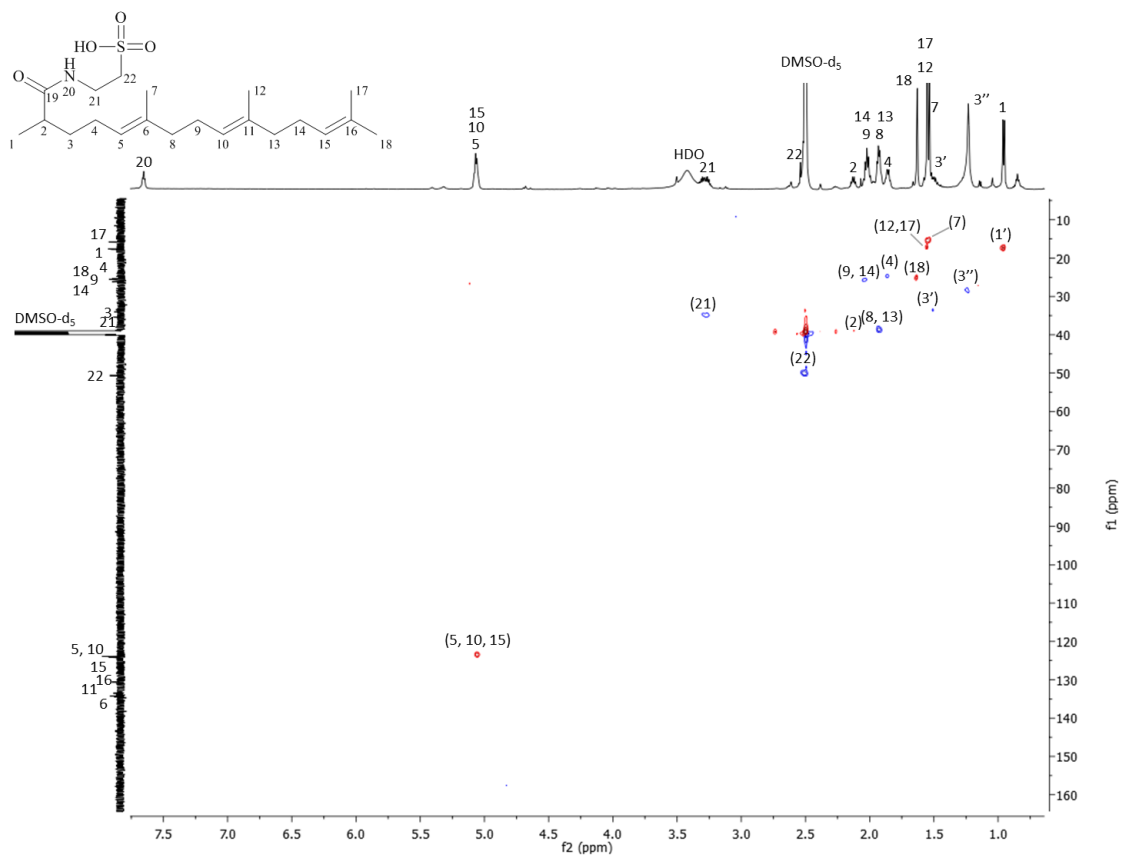


**Figure S6.** HSQC (gc2hsqcse) spectrum of compound **1** in  $\text{dms0-d}_6$ .

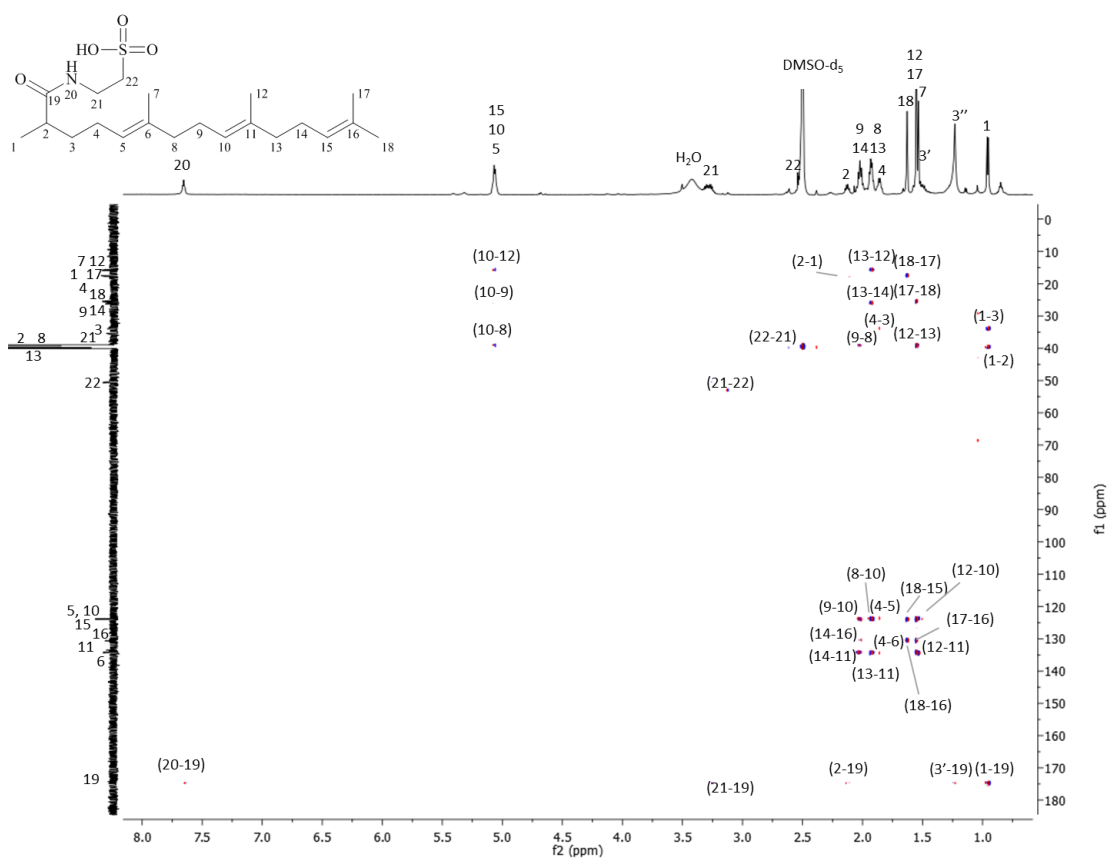


**Figure S7.** HMBC (gc2hmbc) of compound **1** in dmsO-*d*<sub>6</sub>.

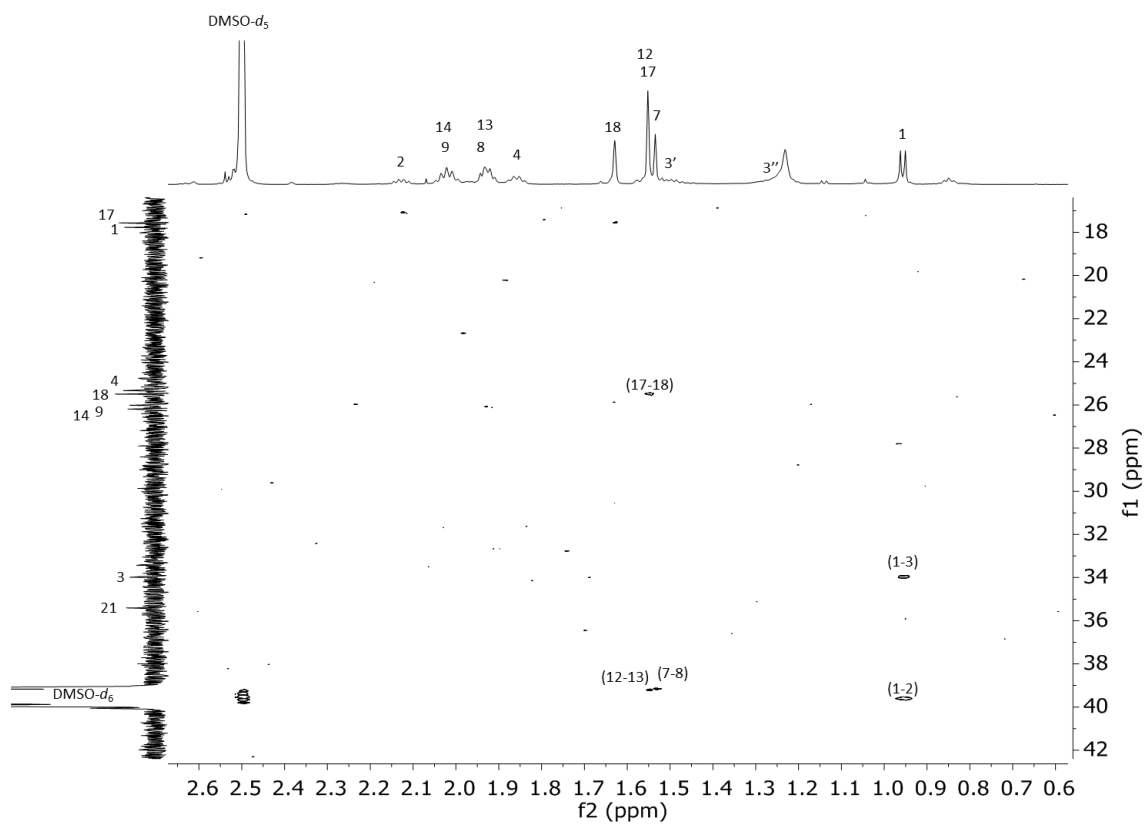


**Figure S8.** High resolution band selective gradient HMBC (bsghmhc) (10-50 ppm) of compound **1** in dmsO-*d*<sub>6</sub>.

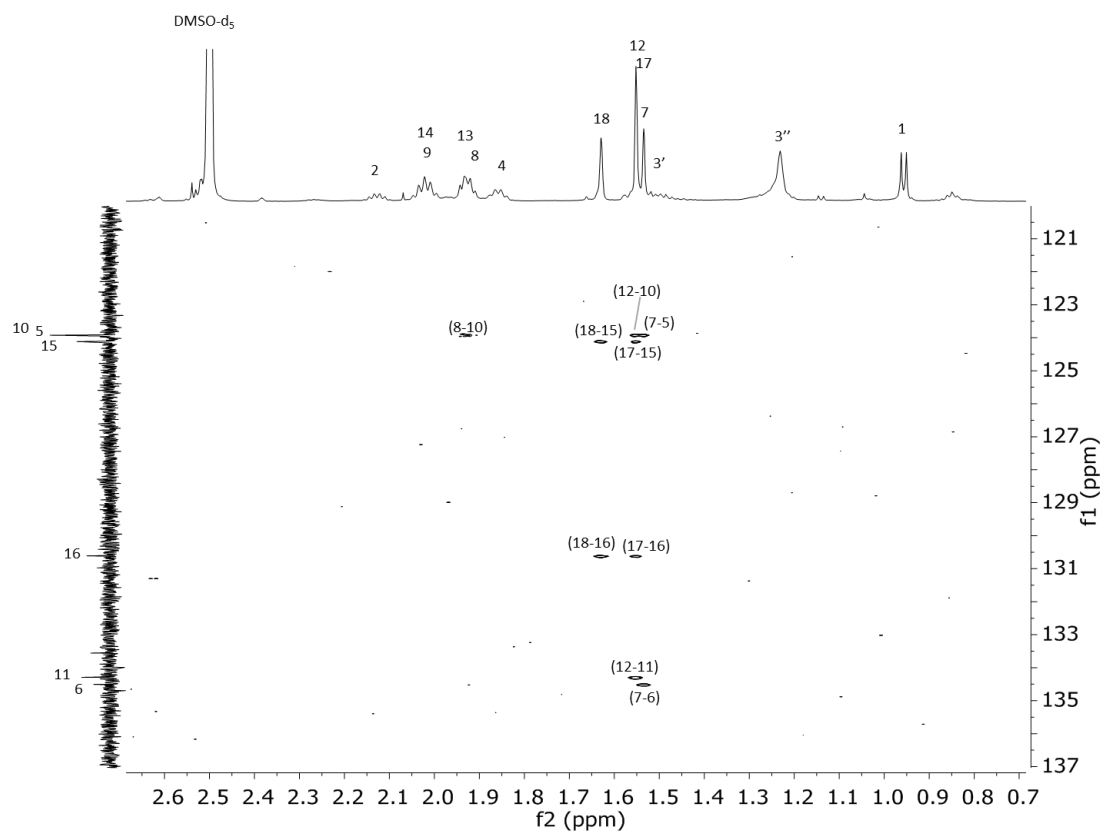


**Figure S9.** High resolution band selective gradient HMBC (bsghmhc) (120-140 ppm) of compound **1** in dmsO-*d*<sub>6</sub>.

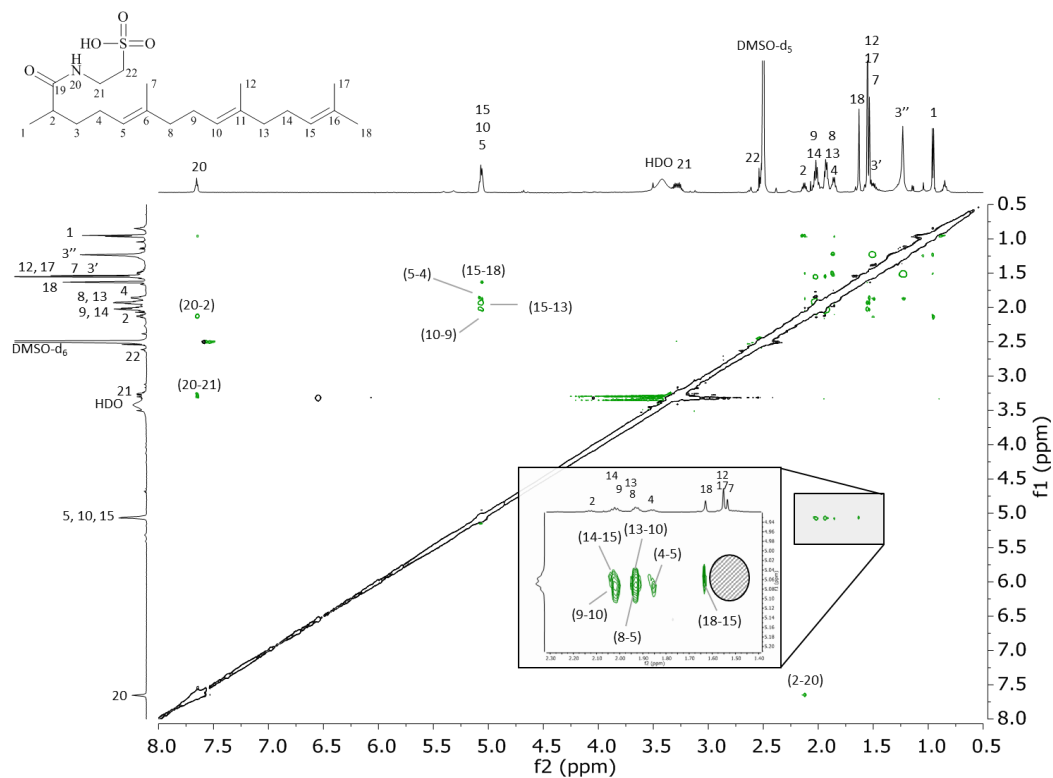


**Figure S10.** 300 ms NOSEY spectrum of compound **1** in  $\text{dms0-d}_6$ . The shaded circle indicates where peaks would have been expected if the double bonds were *cis* instead of *trans*.

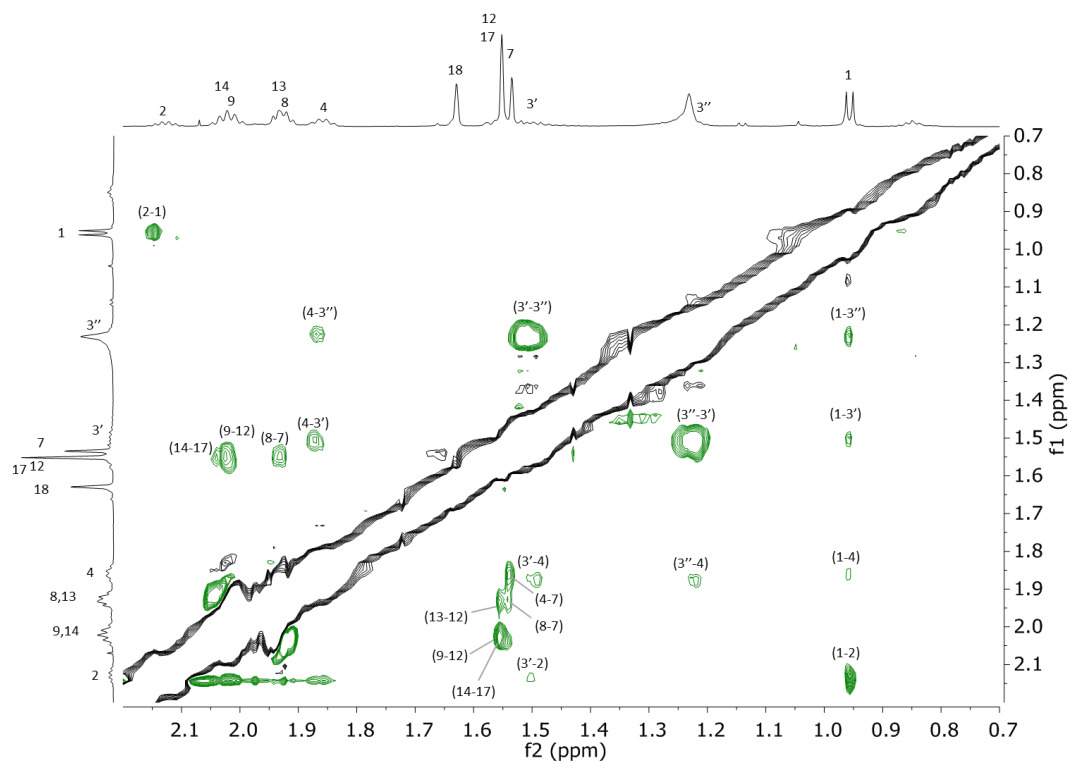


**Figure S11.** 300 ms NOSEY spectrum of compound **1** in  $\text{dms0-d}_6$  (0.5-2 ppm)